Structural, optical, and mechanical characterization of PMMA-MXene composites functionalized with MEMO silane

Ivan Pešić, Miloš Petrović, Marija Vuksanović, Maja Popović, Maja S. Rabasović, Dragutin Šević & Vesna Radojević

Published online: 28 Jan 2023.

Submit your article to this journal ⬈

Article views: 762

View related articles ⬈

View Crossmark data ⬈

Taylor & Francis
Taylor & Francis Group

RESEARCH ARTICLE

OPEN ACCESS   Check for updates

Structural, optical, and mechanical characterization of PMMA-MXene composites functionalized with MEMO silane

Ivan Pešić[a], Miloš Petrović[a], Marija Vuksanović[b], Maja Popović[b], Maja S. Rabasović[c], Dragutin Šević[c] and Vesna Radojević[a]

[a]Faculty of Technology and Metallurgy, University of Belgrade, Belgrade, Serbia; [b]VINČA Institute of Nuclear Sciences - National Institute of the Republic of Serbia, University of Belgrade, Belgrade, Serbia; [c]Institute of Physics Belgrade, University of Belgrade, Belgrade, Serbia

ABSTRACT

Processing and characterization of PMMA-MXene composites were investigated. γ-Methacryloxypropyltrimethoxy (MEMO) silane was used to modify the surface of MXenes and improve the compatibility between MXenes and the polymer. The FTIR analysis revealed the formation of a chemical bond between MXene and MEMO silane, while the XPS analysis confirmed the presence of silicon in the functionalized MXene. PMMA composites with non-functionalized and functionalized MXene were prepared using a solution casting method. Tensile tests showed that, compared to neat PMMA, Young's modulus increased in both composites by 22.1 and 27.6%, respectively. As a result of coupling between the PMMA matrix and the surface-modified MXenes, the tensile strength also increased by about 37%. In addition, optical spectroscopy showed higher absorption for the composite with surface-modified MXenes and short-lived fluorescence with emission intensity sensitive to the crumpling of functionalized MXene nanosheets.

GRAPHICAL ABSTRACT
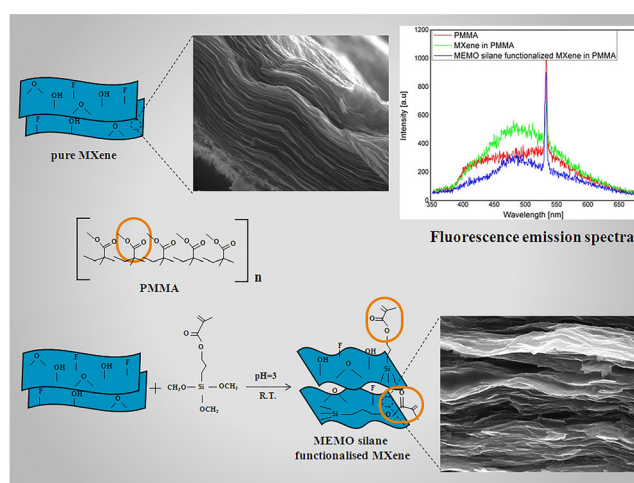
Fluorescence emission spectra

1. Introduction

MXenes are a growing group of 2D materials with a unique combination of properties. MXenes can be synthesized by selective etching of the corresponding MAX phase (top-down) or by chemical vapor deposition (bottom-up). MAX phases are a large family of layered transition metal carbides or nitrides. They can be represented with the general formula $M_{n+1}AX_n$ ($n = 1$–4), where M stands for the transition metal (usually an element from the 3rd to the 5th group of the PTE such as Ti, Zr, V, Nb, Ta, or Cr), A for the element from the 13th or the 14th group (the most common are Al and Si), and X for C or N [1–4]. MXenes have a similar general formula $M_{n+1}X_nT_z$, where M and X have the same meaning, and T represents functional groups attached to the MXene surface. It can be seen from the latter formula that there is a missing A atom which was selectively etched [5,6]. There are over 30 predicted MXene structures, but only some of them

---

CONTACT Ivan Pešić ✉ ipesic@tmf.bg.ac.rs ⊙ Faculty of Technology and Metallurgy, University of Belgrade, Karnegijeva 4, Belgrade, 11120, Serbia.

have been experimentally confirmed [7,8]. Based on their properties, MXenes can be used for different applications such as hydrogen storage, dye absorbents, ion exchange, and antibacterial agents. In addition, MXenes can be used as stable water (or some other) dispersions or as vacuum-filtered films.

Poly(methyl methacrylate) (PMMA) is an acrylate derivative and one of the most interesting industrial thermoplastic polymers. It is weather-resistant, biocompatible, chemically stable, and has good optical transparency from the ultraviolet to the near-infrared regions [9–12]. Polymeric waveguides are mostly made of this polymer because of these properties. Moreover, PMMA-based composites for a wide range of optical and optoelectronic applications can be obtained by embedding optically active media like quantum dots, carbon nanotubes, graphene, nanowires, or single crystals [13–15]. However, one of the drawbacks of this polymer is its brittleness. To enhance its properties, PMMA can be blended with other polymers, or nano- or micro-inorganic fillers can be added to it. The results depend on the type of interaction between the polymer chains and the filler [12,16,17].

Until now, there have been some theoretical descriptions of the mechanical properties of MXene single flakes [18]. In short, MXene single flakes have excellent mechanical properties, very similar to graphene sheets [19], which makes them a good candidate for a load-bearing role in composite materials. According to density functional theory, Young's modulus of the single flake $Ti_3C_2T_x$ MXene is about 0.33 TPa [20]. Since there are a lot of functional groups on the MXene flake surface, they can be modified with different kinds of materials such as nano cellulose, soybean phospholipid, metals (Pt, Ag, etc.), or inorganic compounds (Fe_2O_3, Mn_3O_4) [21–23] to improve or change their properties or just to prevent the oxidation. MXenes can also be incorporated into polymers to create composite materials with enhanced mechanical [24], electrical [25], or optical [26] properties, even with a small concentration of flakes. MXene surface plays a vital role here as well because of its functional groups that can interact with a polymer structure. The problem occurs when MXene functional groups and a polymer are not compatible, which may lead to MXene agglomeration and, consequently, to the deterioration of properties.

MXenes possess promising electron transport properties because of the high density of states at the Fermi level. Thus, they can be considered as materials for various optical applications, like light harvesting materials, and as functional mediums in polymer composites in optical, electromagnetic interference (EMI) shielding, or sensing applications [25,27–30]. The optical properties of MXenes are influenced by way of their surface termination. One of the possible sites for surface termination is on top of transition metal atoms; the second is between top metal atoms, and the third is between stacking X-atom layers [28,30].

The research interest in MXene polymer composites increased over the past few years. It can be concluded that the processing method also influences the properties of polymer composites with MXene [31–34]. Highly transparent $Ti_3C_2T_x$ MXene film on flexible PET substrate was prepared by Ying et al. [33]. The processing by *in situ* polymerization was also performed with very good results, and the hybrid nanocomposite of PMMA with MXene/ZnO nanoparticles with improved dielectric properties was obtained [34]. Melt blending proved to be a suitable method when working with a thermoplastic polymer matrix, for example, for preparing thermoplastic polyurethane (TPU) nanocomposites with homogeneously dispersed Ti_3C_2 MXene nanosheets [32]. All these methods were developed to achieve composites with high performances.

Various MXene modifications may lead to better compatibility between the flakes and the polymer matrix and suppress the aggregation of MXene nanosheets, as evidenced by the use of polyethylene glycol (PEG) [35], dopamine [33], or aniline [34]. There is also a well-described method of MXene functionalization with amino silane [36], which can serve as the basis when utilizing silanes.

The idea to incorporate MXenes in PMMA originated from our attempts to produce an optically sensitive transparent thin film. There are only a few studies of PMMA-MXene nanocomposites [37], including our previous work [38] and the synthesis of specific MXene structures using PMMA as a template [35]. To our knowledge, there were no previous attempts to synthesize polymer composites with MXenes functionalized with silane. γ-Methacryloxypropyltrimethoxy (MEMO) silane was chosen for MXene functionalization because of its very similar structure to PMMA, which results in better compatibility and stronger interfacial bonding in the composite [36,37].

In our research, we analyzed the impact of functionalized MXenes on the optical and mechanical properties of the PMMA. Two types of composites were prepared: the first one, where the MXenes were directly added to PMMA, and the second one, where the MXenes were functionalized with MEMO silane before they were added to PMMA. The obtained composites were tested in order to determine Young's modulus and tensile strength and prove that the optical properties of MXenes are preserved when added to PMMA.

2. Experimental section

2.1. Materials

For the preparation of Ti_3C_2 MXene, concentrated HCl (Fisher Scientific UK) and LiF (325 mesh powder Alfa Aesar) were used. γ-Methacryloxypropyltrimethoxy (MEMO) silane (Dynsasylan MEMO) was used to functionalize MXenes. DMF was purchased from Sigma Aldrich. Dimethyl sulfoxide (DMSO) was purchased from Fisher Scientific UK. PMMA pellets (Acryrex®, Chi Mei Corporation, Taiwan) were used to prepare the composites.

2.2. Preparation of delaminated Ti_3C_2 MXene

Ti_3C_2 MXene was prepared by etching the Ti_3AlC_2 MAX phase using LiF/HCl method. The powdered MAX phase was gradually added into a mixture of LiF and concentrated HCl. After 24 h at 35 °C, the dispersion was rinsed with DI water until pH 5, and the supernatant turned black. The centrifuge tube was shaken by hand for 1 min after adding water during the rinsing procedure. After the last washing step, sediment was again dispersed in DMF and sonicated for 1 h under argon bubbling. Finally, the obtained dispersion was centrifuged for 1 h at 3000 rpm, and the supernatant was collected.

2.3. Modification of MXene with MEMO silane

MEMO silane was first hydrolyzed in 50 ml of water/ethanol solution at room temperature for 1 h, and the pH was adjusted with acetic acid [37].

MEMO silane functionalized MXene was prepared through a similar method as pure MXene. Ti_3C_2 MAX phase was etched using LiF/HCl method. The powdered MAX phase was gradually added into a mixture of LiF and concentrated HCl. After 24 h at 35 °C, the dispersion was rinsed with DI water until pH 5, and the supernatant turned black. The centrifuge tube was shaken by hand for 1 min after adding water during the rinsing procedure. The obtained sediment was dried for 1 h at 70 °C and mixed with DMSO for 18 h in a magnetic stirrer. After the mixing, sediment was separated from the excess DMSO by centrifugation. Afterward, it was redispersed in deionized water and sonicated for 1 h under argon bubbling. Finally, the obtained dispersion was centrifuged for 1 h at 3000 rpm, and the supernatant was collected.

The mass ratio of MEMO silane to MXene was 3:1. Hydrolyzed MEMO silane and MXene supernatant were mixed with a magnetic stirrer. The obtained mixture was centrifuged for 10 min at 4000 rpm to sediment unreacted silane. The supernatant was then vacuum filtered to get the thin film of functionalized MXene, and used in further synthesis.

2.4. Sample preparation

Three series of samples were prepared: pure PMMA, PMMA with unmodified MXenes (PMMA-MX), and PMMA with MEMO silane-modified MXenes (PMMA-MXS).

Series 1 - PMMA

A pure PMMA matrix was prepared by dissolving the PMMA pellets in dimethylformamide (DMF) for 24 h in a magnetic stirrer. The solution was then poured into Teflon molds and left partially covered in the dryer for another 24 h at 65 °C.

Series 2 - PMMA-MX

The supernatant was used as a solvent for the series. PMMA pellets were put into the supernatant and left in the magnetic stirrer for 24 h. The concentration of MXenes in the composite was 1 wt%. The solution was poured into Teflon molds and dried for 24 h at 50 °C, followed by 24 h in a vacuum drier.

Series 3 - PMMA-MXS

PMMA was dissolved in DMF for 24 h in a magnetic stirrer. After that, the previously made thin film was measured, chipped, and added to the solution to obtain the concentration of 1 wt% of the functionalized MXene in PMMA. Next, the solution was treated in an ultrasonic bath for several minutes to break down the chips, followed by stirring for another 24 h. The solution was then poured into Teflon molds and left in the oven at 65 °C overnight.
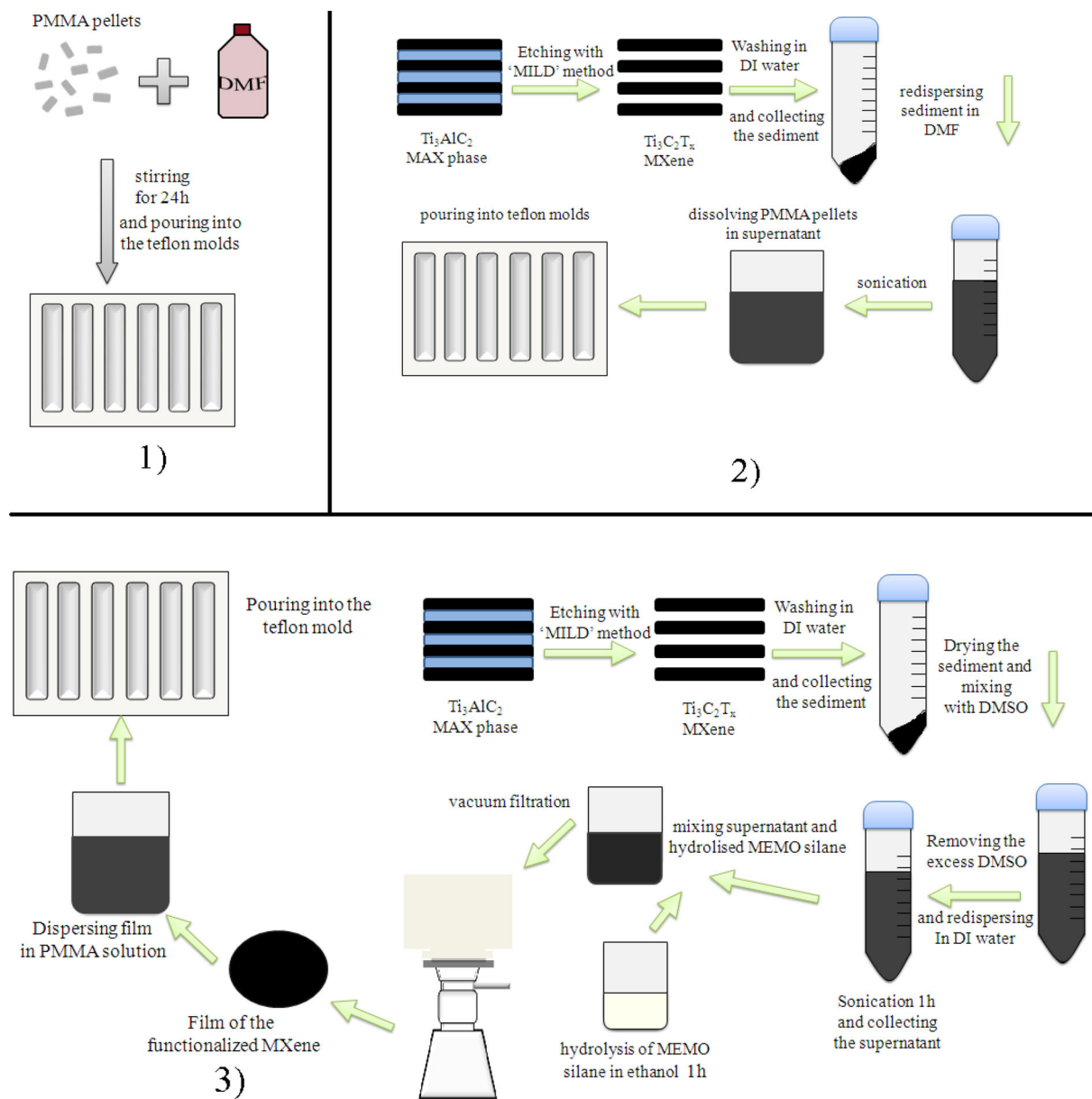
The schematic representation of the experiment is shown in Figure 1.

### 2.5. Material characterization

FTIR spectra of functionalized MXene and composites were collected through single-beam Fourier-Transfer Infrared Spectroscopy (FTIR) using a Nicolet 6700 spectrometer.

SEM images were obtained by using FESEM Tescan MIRA 3 XMU electron microscope.

Tensile testing was performed at room temperature with the Shimadzu EZ-LX universal testing instrument equipped with a 5 kN load cell. The machine resolution was ±0.5% of the indicated value (within 1/500 to 1/1 of load cell rated capacity), and crosshead position detection accuracy was 0.1%. The samples (12 mm wide, 60 mm long, and 0.5 mm thick) were tested at a 3 mm/min speed. All the samples were conditioned at room temperature and

Figure 1. Schematic representation of the experiment: (1) preparation of PMMA, (2) preparation of unmodified MXene in PMMA (PMMA-MX), and (3) preparation of MEMO silane-modified MXene in PMMA (PMMA-MXS).
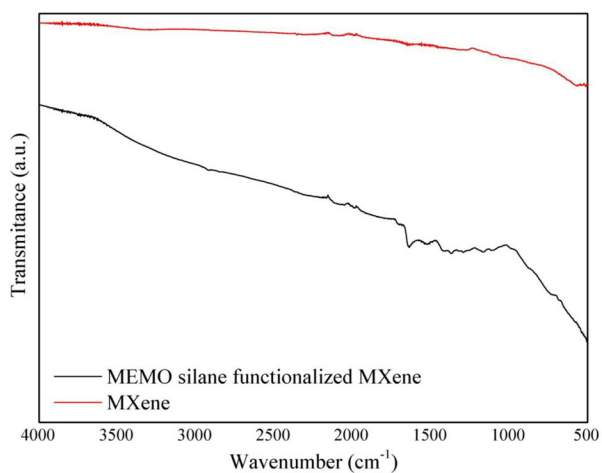

Figure 2. FTIR spectra of MEMO silane functionalized MXene and pure MXene.

in a desiccator for 48 h before measurements. Three identical samples were tested for each series.

XPS analysis of the samples was carried out on the SPECS Systems with XP50M X-ray source for Focus 500 and PHOIBOS 100 energy analyzer using a monochromatic Al Kα X-ray source (1486.74 eV) at 12.5 kV and 12 mA. All samples were fixed onto an adhesive copper foil to provide strong mechanical attachment and good electrical contact. All survey XPS spectra (0–1300 eV BE) were recorded with a constant pass energy of 40 eV, energy step of 0.5 eV, and dwell time of 0.2 s, while high-resolution XPS spectra of the corresponding lines were taken with a pass energy of 20 eV, energy step of 0.1 eV and a dwell time of 2 s.

The optical characteristics of MXenes were measured using a time-resolved laser-induced optical spectroscopy system. It is based on Nd-YAG Vibrant

NANOCOMPOSITES 219
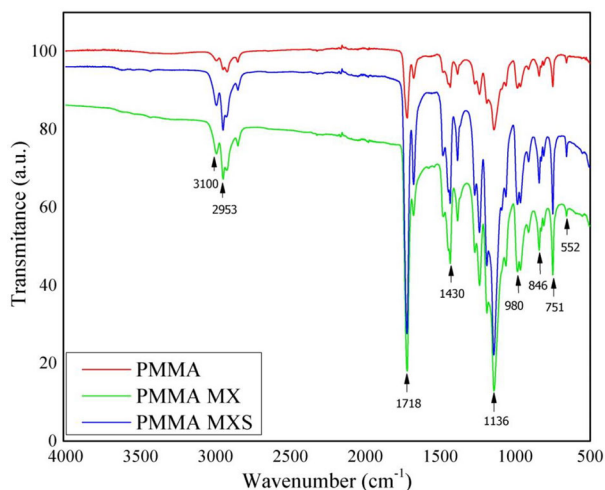
Figure 3. FTIR spectra of PMMA, PMMA-MX, and PMMA-MXS.

OPO (Optical Parametric Oscillator) laser as an excitation source. The OPO output is continuously tunable in the range between 320 and 475 nm. The fourth harmonic (266 nm) and the second harmonic (532 nm) outputs are also available. The time duration of the laser pulse is about 5 ns, and its repetition rate is 10 Hz. The samples' time-resolved emission spectra were obtained by using the Hamamatsu streak camera system equipped with the spectrograph. Absorbance spectra were obtained using the Ocean Optics HR2000 spectrometer. The samples were excited by a 12 V, 55 W halogen light bulb.

3. Results and discussion

The Fourier transformation infrared spectroscopy (FTIR) was used to confirm the functionalization of
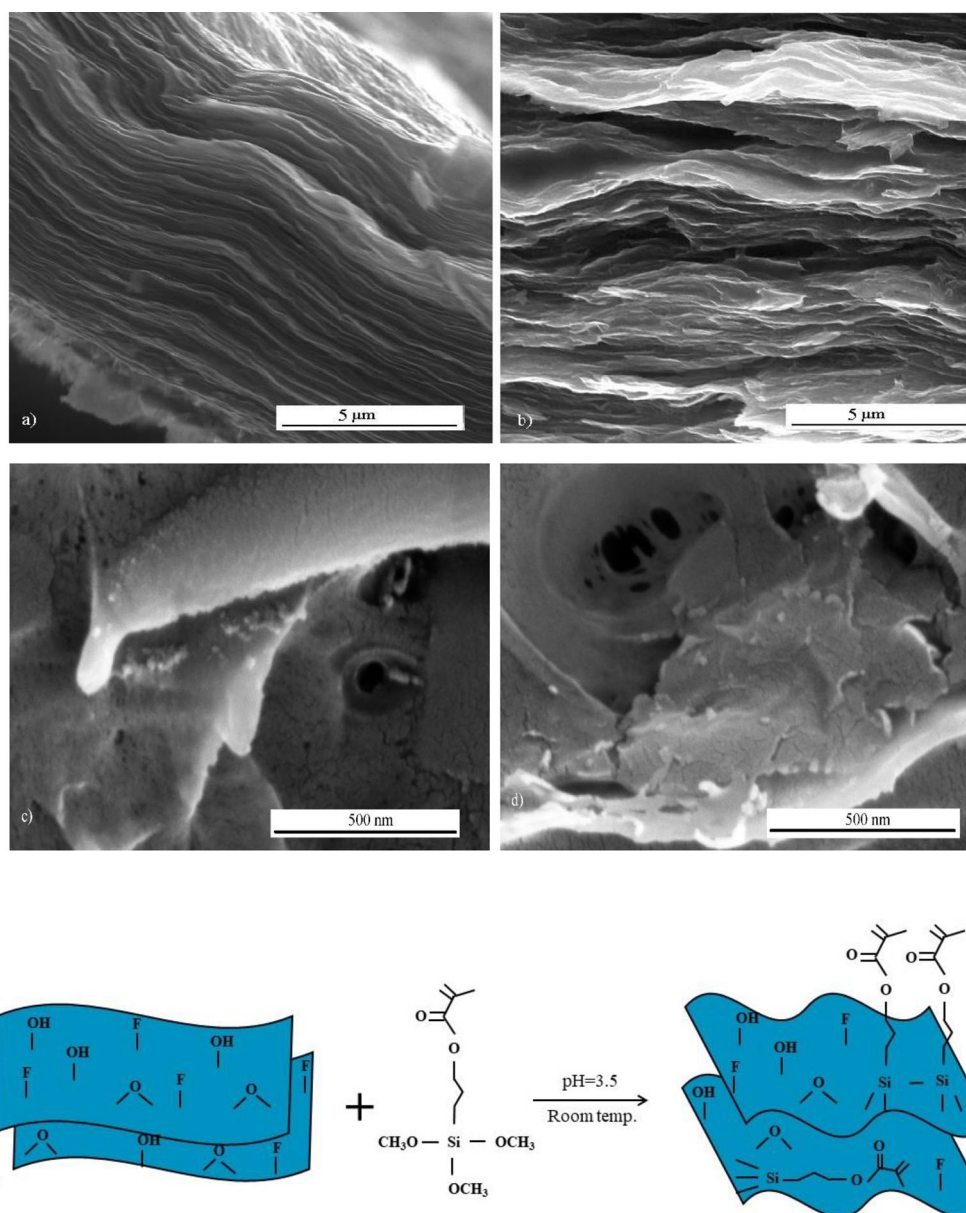
Figure 4. SEM images of (a) MXenes and (b) MEMO silane functionalized MXenes, (c) cross-section of PMMA-MX, (d) cross-section of PMMA-MXS and (e) schematic representation of the pristine $Ti_3C_2T_x$ flakes reacting with the γ-methacryloxypropyltrimethoxy coupling agent.

MXene with MEMO silane (Figure 2). The characteristic broad peak around 3500 cm^{-1}, which corresponds to hydroxyl groups or entrapped water, can be seen in the spectrum of unmodified MXene. The disappearance of this peak in the spectrum of modified MXene can be attributed to the termination of OH groups by silanol groups of MEMO silane [36,39].

FTIR measurements for the composite samples are shown in Figure 3. Characteristic peaks for PMMA occur at 1718 cm^{-1} ν (C=O) and 1430 cm^{-1} ν (C–O). The bands at 2953 cm^{-1} correspond to the C–H elongation of the methyl group (CH$_3$). The peak at 1136 cm^{-1} corresponds to the vibrations of the ester group C–O [39]. The peak at 980 cm^{-1} corresponds to the ester bonds, and peaks at 751 and 846 cm^{-1} represent (C–C) stretching [40]. Spectra of series with MXene have a new peak that corresponds to Ti–O stretching vibration and shifts to 552 (596) cm^{-1} [41]. Also, a new broad feature centered at ~3100 cm^{-1} is present in these spectra and can be attributed to the Ti–OH bond [42].

Scanning electron microscopy (SEM) was employed to examine the structure of the particles used in the experiment. Both MXenes and MEMO silane functionalized MXenes were vacuum filtered to obtain the samples for the microscope. Results are shown in Figure 4.

At first glance, a compact structure is observed in both cases. It is assumed that nanosheets were stacked during vacuum filtration. On the other hand, as shown in Figure 4b, which represents functionalized MXenes, the structure is looser and less compact. Since the pH of hydrolyzed MEMO silane used in synthesis was 3, this caused the 'crumpling' of MXene flakes, as reported in [43]. In addition, after functionalization, the silane molecules bonded to the flakes' surface in the perpendicular direction, which also leads to an enlarged spacing between MXene layers [43,44] and is, along with the crumpling, represented in Figure 4.

In order to confirm our assumptions about the improved compatibility between functionalized MXenes and PMMA, we analyzed the SEM images of both types of composites, which are presented in Figure 4c and d, respectively. Figure 4c represents the cross-section of the PMMA-MX sample.
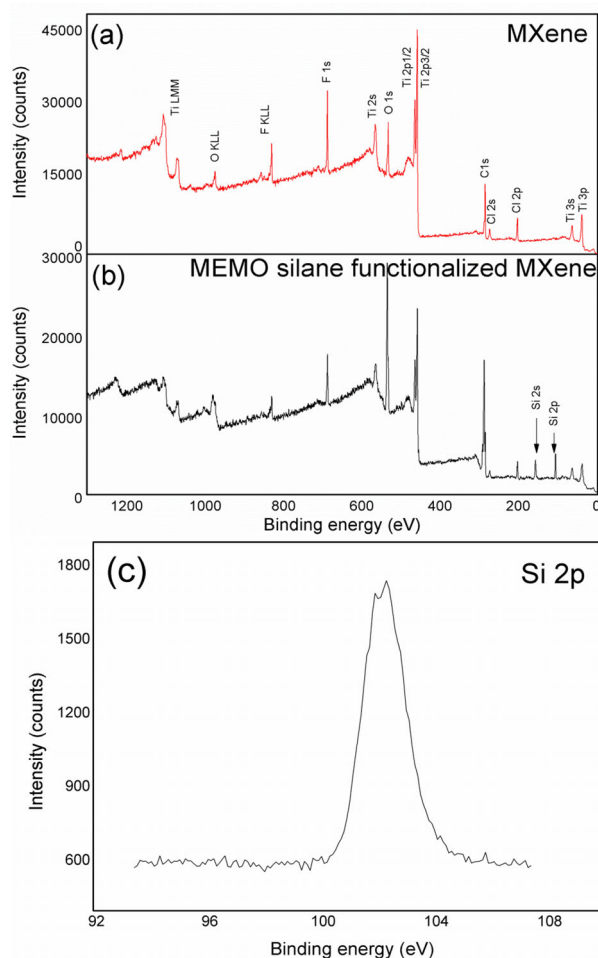
Figure 6. XPS survey spectra of (a) MXene and (b) MEMO silane functionalized MXene, and (c) high-resolution XPS spectrum of Si 2p line of MEMO silane functionalized MXene.
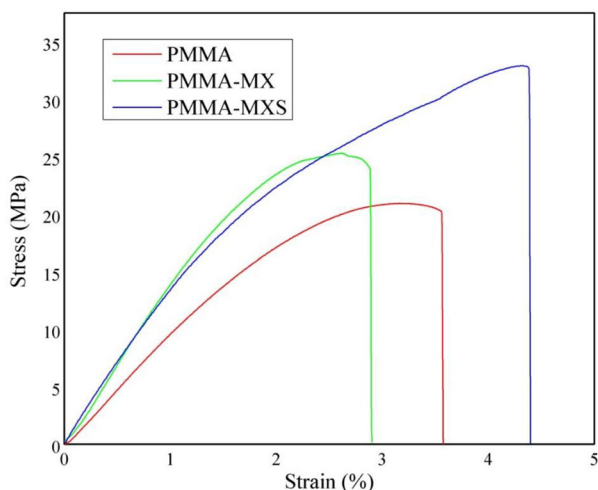

Figure 5. Stress vs. strain diagram for the PMMA, PMMA-MX, and PMMA-MXS.

Table 1. Average values of Young's modulus, tensile strength and strain at break, with corresponding standard deviations (SD).

Series	Young's modulus (MPa)	SD (Mpa)	Tensile strength (Mpa)	SD (MPa)	Strain at break (%)	SD (%)
PMMA	1015.22	182.29	21.98	1.48	3.63	0.67
PMMA-MX	1235.81	192.21	23.96	1.88	2.33	0.41
PMMA-MXS	1291.75	164.68	30.05	4.06	3.96	0.50

Clusters of MXene nanoparticles can be observed due to the rigorous mixing of the polymer solution. On the other hand, no noticeable agglomeration can be observed in the cross-section of the PMMA-MXS sample (Figure 4d). That is, MXene nanoparticles are more evenly distributed.

The representative curves from the tensile test of all three series are shown in Figure 5 and summarized in Table 1.

From the shapes of tensile curves, it can be seen that Young's modulus, calculated as the slope of the linear section of the stress–strain curve in the 0.5–2.5 MPa stress range, increases for both PMMA-MX and PMMA-MXS. The strain at break, however, is lower for PMMA-MX. This can be explained by the incompatibility between the MXene surface and PMMA, which leads to MXene flakes serving as stress concentrators and causing micro ruptures during deformation. Better bonding between MEMO silane functionalized MXene and PMMA is achieved in the PMMA-MXS composite, which results in improved load transfer from the matrix to reinforcements. As a result, the strain at break and tensile strength increase for PMMA-MXS, and consequently, its toughness improves.

The average values of mechanical properties determined by tensile tests, along with corresponding standard deviations (s.d.), are shown in Table 1. Compared to the results of some other MXene-polymer nanocomposites and PMMA nanocomposites with other nanoparticles, our materials follow the trend of the increased values of Young's modulus and tensile strength as obtained in [45–47]. Looking at the relative improvement of Young's modulus, in this work, an increase of 22.1% for PMMA-MX and 27.6% for PMMA-MXS were achieved, which is in accordance with other studies, e.g. an increase of 38.9% in [45] and 33% in [47]. The increase in tensile strength was 9% for PMMA-MX and almost 40% for PMMA-MXS. Compared with other MXene-polymer composites with a similar wt% of filler content, thermoplastic polyurethane (PTU) with 1 wt% has a 25% increase in tensile strength [48], while for 0.5 wt% of MXenes in Waterborne polyurethane and Ultrahigh molecular weight polyethylene the increase was 25 and 65%, respectively [48]. For nanocomposites with 1 wt% of graphene oxide in PTU and 5.4 wt% in PVA, the increase of tensile strength was 40 and 87%, respectively [49,50]. In addition, the theoretical prediction of the modulus of elasticity can be calculated using Halpin–Tsai's micromechanical model leading to the value of 2152 MPa, which is comparable to the values that we observed for PMMA-MX and PMMA-MXS samples.

In order to express the reliability of the results of mechanical testing, standard deviation and measurement uncertainty were calculated. Measurement accuracy analysis for tensile strength (TS) was performed with the method defined by Klysz [50,51]. Based on machine accuracy, the standard uncertainty for TS was calculated as $u(TS) = 0.18$ MPa [52]. For strain, the standard uncertainty was calculated as $u(Str) = 0.21\%$ [52]. Uncertainty of measurements is a parameter for error probability distribution in the context of instrument accuracy's influence. The uncertainty of measurements is lower than the standard deviation, as can be seen from Table 1, so the instrument's influence on the error can be considered as low. Actually, both the standard deviation and uncertainty of the measurements are considerably influenced by the number of samples in a testing procedure [52].

Survey spectra of MXene and functionalized MXene with MEMO silane are presented in Figure 6a and b, respectively. The main photoelectron lines of Ti, O, and C constituting elements are clearly observed and marked together with their Auger lines. The photoelectron lines detected at around
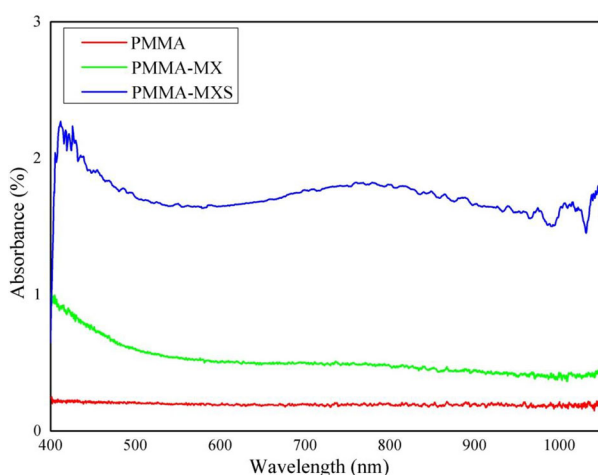

Figure 7. Absorbance spectra of PMMA, PMMA-MX, and PMMA-MXS.

Figure 8. The optical transparency of PMMA, PMMA-MX, and PMMA-MXS samples.

685, 270, and 200 eV belong to F1s, Cl2s, and Cl2p, respectively, which originate from the preparation procedure of Ti$_3$C$_2$ MXene using the LiF/HCl method. It was found that after functionalization of MXene with MEMO silane (Figure 7b), the additional lines that correspond to silicon (Si 2s and Si 2p lines, respectively), which are marked with arrows, were observed at about 154 and 102 eV. The region of Si 2p recorded in better resolution is presented in Figure 6c, confirming the successful functionalization of MXene with MEMO silane.

Absorbance spectra of PMMA, PMMA-MX, and PMMA-MXS are shown in Figure 7. Due to the low signal levels in UV and IR regions, corresponding parts of measured spectra are very noisy. Therefore, the truncated wavelength range is presented in Figure 7 of spectra that were measured originally in the range between 300 and 1100 nm. Absorbance spectra of MXene samples have similar shapes as absorbance spectra obtained by Maleski et al. [53], where the spectrum of MXene on the sapphire surface was presented. In the 300–400 nm range, the spectrum is with a lot of noise because of the dispersion of MXenes in PMMA and some signal attenuation. It can be seen that functionalized MXene in PMMA shows higher absorbance in the 800 nm region, similarly to [53], while for pure

MXene, absorbance in this region is lower. The absorbance of PMMA is almost flat in the entire region. The absorption peak at 800 nm observed in PMMA-MXS is ascribed to the inherent out-plane interband transitions [53].

To show the changes in the optical appearance of the composites, we photographed them on a piece of paper, along with neat PMMA, so they could be observed together and compared. The resulting image is shown in Figure 8.

Emission intensity (integrated-in-time) of time-resolved optical spectra of PMMA, MXene in PMMA, and MEMO silane functionalized MXene in PMMA using the 266 nm excitation are shown in Figure 9. The very strong peak at 532 nm actually corresponds to spectrometer diffraction grating second-order "ghost" of laser excitation at 266 nm. Because of their relatively small absorption, as MXene materials have moderate quantum yield (8.9% in Desai et al. [54]), they are also characterized by small fluorescence intensity. As shown in [34], MXene materials have wideband fluorescence emission in the 400–600 nm range. Regardless, the emission peak of PMMA-MX is the highest and slightly red-shifted to higher wavelengths. However, the peak of PMMA-MXS again blue shifts and appears at nearly the same wavelength as in the spectrum of neat PMMA. This influence of silane modification was already observed in our earlier work [38] and can be attributed to the silane modification influencing a better spatial organization of modified MXenes in the polymer matrix. The MXene fluorescence spectra have shapes very similar to spectral shapes presented in Desai et al. [54], where MXene nanosheets were used for selective and sensitive fluorescence detection of Ag$^+$ and Mn^{2+} ions. In this research, the disturbance of MXene nanosheets with the embedding of these ions also occurred. As shown in Figure 10, which represents streak images of time-resolved spectra of PMMA, PMMA-MX, and PMMA-MXS, MXene fluorescence is very short-lived. It lasts only as long as the laser pulse lasts. Therefore, with the laser excitation duration of 5 ns and the repetition rate of 10 Hz, we obtained relatively small intensities of
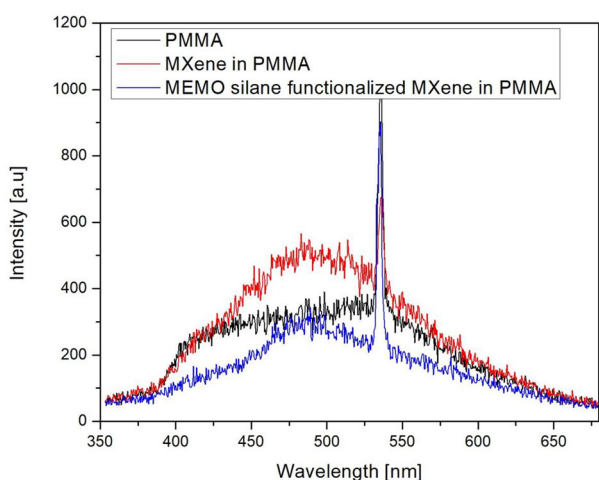
Figure 9. Emission intensity (integrated-in-time) of time-resolved optical spectra of PMMA, PMMA-MX, and PMMA-MXS.
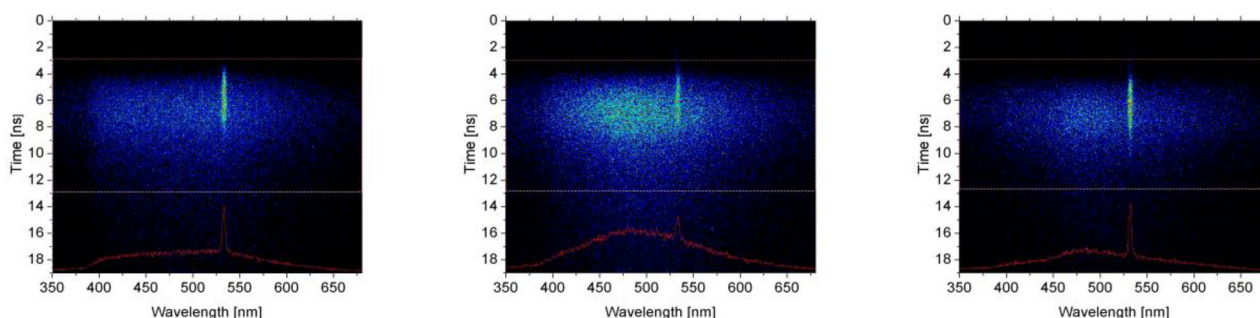
Figure 10. Streak images of time-resolved optical spectra of (a) PMMA, (b) PMMA-MX, and (c) PMMA-MXS.

MXene fluorescence compared to [54], where continuous excitation was used.

Presented results suggest that the fluorescence emission is sensitive to the surface modification of MXene and the crumpling of MXene nanosheets. This results in fluorescence quenching, that is, the decreasing of the fluorescence intensity in PMMA-MXS that can be associated with the MXene-silane bonding. The broad absorption properties of MXenes in the 400–1200 nm range and their intrinsic fluorescence quenching ability make them a promising material as a quencher in fluorescence resonance energy transfer (FRET) [55,56]. Thus, our PMMA-MXS thin film can potentially be used as a biosensing element in fluorometric assays.

4. Conclusion

A new type of MXene-based PMMA composites with improved toughness was developed *via* a simple solution casting method. To improve the bonding between the reinforcement and the polymer matrix, MXenes were functionalized with MEMO silane. Composites with unmodified and functionalized MXenes were processed, and structural, optical, and mechanical properties were investigated and analyzed in order to pave the way for understanding the significance of MEMO silane addition to the MXenes. Functionalization was confirmed with the comparative FTIR analysis of neat and functionalized MXenes and the XPS survey spectra. SEM images and tensile tests confirmed improved compatibility of functionalized MXenes with PMMA, as higher tensile strength, strain at break, and modulus of elasticity were obtained in PMMA-MXS. Optical characterization of composites revealed that functionalized MXenes in PMMA showed higher absorption in some parts of the visible spectrum. The silane modification influences a better spatial organization of modified MXenes in the PMMA matrix, resulting in better fluorescence quenching and leading to the potential use of PMMA-MXS thin films as enzyme reaction sensors. This research helps to disclose some of the properties of this type of nanocomposites that are novel and are yet to be fully understood.

Disclosure statement

No potential conflict of interest was reported by the author(s).

Funding

Notes on contributors

Ivan Pešić, Junior researcher, Faculty of Technology and Metallurgy, University of Belgrade. Born on the 7th of February 1994. He received his B.Sc., and M.Sc. degrees in material science from the University of Belgrade, Serbia, in 2017 and 2018, respectively. In 2018 he enrolled in Ph.D. studies at the Faculty of Technology and Metallurgy, University of Belgrade, and was engaged in the project "Development of equipment and processes for obtaining polymer composite materials with predefined functional properties" as a junior researcher. His field of interest includes 2D nanomaterials-MXenes, polymer composites with MXenes, and the functionalization of MXenes.

Dr Miloš Petrović, Assistant Professor, Faculty of Technology and Metallurgy, University of Belgrade. He received his B.Sc., M.Sc., and Ph.D. degrees in electrical engineering from the University of Belgrade, Serbia, in 2003, 2006, and 2016, respectively. In 2004 he worked as a Development Engineer in Pupin Telecom DKTS. From 2005 to 2007, he was a Research Assistant at the Faculty of Electrical Engineering, University of Belgrade, Serbia. Since 2008, he has been working at the University of Belgrade, Faculty of Technology and Metallurgy, Serbia, where he currently teaches courses in Technical Physics, Circuit and Electronics and Measurements in Technology. He is the author of two university textbooks, more than 40 articles and several technical and developmental solutions. Dr Petrović has participated in several national and international research and innovation projects. His current research interests include sensors, composite materials and materials testing. His previous research interests were in the area of highperformance switching and routing.

Dr Marija Vuksanović was born in Uzice, Serbia. She graduated in 2005th at the Faculty of Technology and Metallurgy, University of Belgrade. She defended a master thesis under the title: "Possibilities for improving the thermomechanical properties of refractory material with the addition of alumina-based ceramic fibres" at the Faculty of Technology and Metallurgy, University of Belgrade, Department of Materials Engineering in 2008. She defended PhD thesis with a topic "Morphological analysis of damage on refractories exposed to thermal shock". She promoted as Doctor of Philosophy for the field of Chemistry and Chemical technology. She is engaged in national project TR34011 titled: "Development of equipment and process of obtaining polymeric composite materials with predefined functional properties", financed by the Ministry of Education, Science and Technological Development of the Republic of Serbia.

Dr Maja Popović was born on the 17th of May 1977. She is employed as Senior Research Associate in the Department of atomic physics in the "Vinča" Institute of Nuclear Sciences - National Institute of the Republic of Serbia, University of Belgrade. After graduation at the Faculty of Physical Chemistry of the University of Belgrade, in 2004 she started working as Reseacrh Trainee in the Vinča Institute of Nuclear Sciences in the Department of atomic physics where she has remained

until now. Her main research fields include: solid state physics, physics of metallic layers and metal-nitrides thin films, ion beam interaction with solids, chemical analysis of solid surfaces, plasmonic metal nanoparticles – synthesis by noble metal ion beam. She published more than 54 papers in international scientific journals (Hirsch index: 11, Total citations (without self-citations): 338 (as of May 2021)). She is reviwer for more than 10 scientific journals. She participated in more than 10 international and national projects. She has a successful international colaborations with Georg-August-Univerisität Goettingen (Germany), Slovak University of Technology in Bratislava, Faculty of Materials Science and Technology in Trnava, Advanced Technologies Research Institute and with Physikalisch-Astronomische Fakultät, Friedrich-Schiller-Universität Jena (Germany).

Dr Maja S. Rabasović is an Associate Research Professor at the Institute of Physics, Belgrade, Serbia. She received her PhD degree from the Physics Department of the University of Belgrade, in 2013. Her current research interests include electron atom collision processes, laser-induced breakdown spectroscopy, fluorescence spectroscopy and imaging, upconversion, nanomaterials, phosphors, machine learning.

Dr Dragutin Šević received the B.S., M.S, and Ph.D. degrees in electrical engineering from the Faculty of Electrical Engineering, Belgrade, in 1984, 1991, and 1995, respectively. In 1984 he joined the Institute of Physics, Belgrade, where he is now Research Professor. From 1998 he is a member of Laboratory for Atomic Collision Processes. His current research interests are: Photonics, Machine Learning, Atomic physics, Digital Signal processing, Data acquisition, Plasma physics.

Dr Vesna Radojević (female), Professor at FTM received Ph.D. degrees in materials science from the University of Belgrade, Serbia, in 2000. She worked at the Institute Mihailo Pupin from 1985 to 1987. Since 1987, she is in the Department of Construction and Advanced Materials, Faculty of Technology and Metallurgy, University of Belgrade, Serbia, where she is currently a Full Professor and Head of Departement. In the period 2004–2006, she was appointed the Vice Dean for Bachelor and Master Studies at the same Faculty. From 2009 to 2012, she served as the President of the Professional Ethic Committee of the University of Belgrade. From 2008 to 2015, she was Reviewer/expert for Accreditation Committee of the Ministry of Education, Science and Technological Development (Bachelor, Master and PhD studies). She is the author of two books, more than 75 SCI articles and more than 35 technical solutions and participant of 6 international and 12 national projects. ORCID 0000-0001-9301-3983, Scopus Author ID 56343867900. Her research interests include processing and characterization of functional composite materials (bio composites, dental composites, construction composites and optoelectronic composites, materials for energy storage) at micro to nano level. She has been awarded several Silver plaques for technological innovation.

References

1. Anasori B, Gogotsi Y. 2D Metal carbidesand nitrides (MXenes) structure, propertiesand applications. Switzerland: Springer, 2019.

2. Naguib M, Mashtalir O, Carle J, et al. Two-dimensional transition metal carbides. ACSNano. 2012; 6(2):1322–1331.

3. Naguib AM. MXenes: a new family of two-dimensional materialsand its application as electrodes for Li-ion batteries. Philadelphia: Drexel University, 2014.

4. Barsoum MW, Gogotsi Y, Abdelmalak MN, et al. Compositions comprising free standing two dimensional nanocrystals US Patent 9,193,595, 2015.

5. Anasori B, Xie Y, Beidaghi M, et al. Two-dimensional ordered double transition metals carbides (MXenes). ACS Nano. 2015;9(10):9507–9516.

6. Anasori B, Lukatskaya MR, Gogotsi Y. 2D metal carbides and nitrides (MXenes) for energystorage. Nat Rev Mater. 2017;2(2):16098.

7. Chaudhari NK, Jin H, Kim B, et al. MXene: an emerging two-dimensional material for future energy conversion and storage applications. J Mater Chem A. 2017;5(47):24564–24579.,

8. Khazaei M, Ranjbar A, Arai M, et al. Electronic properties and applications of MXenes: a theoretical review. J Mater Chem C. 2017;5(10):2488–2503.

9. Sahoo PK, Samal R. Fire retardancy and biodegradability of poly(methyl methacrylate)/montmorillonite nanocomposite. Polymer Degrad Stabil. 2007; 92(9):1700–1707.

10. Khalaf AI, Assem Y, Yehia AA, et al. Synthesis and characterization of hybrid clay/poly (N,N dimethylaminoethyl methacrylate) nanocomposites. Polym Compos. 2016;37(10):2950–2959.

11. Unnikrishnan L, Mohanty S, Nayak SK, et al. Preparation and characterization of poly(methyl methacrylate)–clay nanocomposites via melt intercalation: the effect of organoclay on the structure and thermal properties. Mater Sci Eng A. 2011; 528(12):3943–3951.

12. Pang L, Shen Y, Tetz K, et al. PMMA quantum dots composites fabricated via use of pre-polymerization. Opt Express. 2005;13(1):44–49.

13. Feizi S, Zare H, Hoseinpour M. Investigation of dosimetric characteristics of a core–shell quantum dots nano composite (CdTe/CdS/PMMA): fabrication of a new gamma sensor. Appl Phys A. 2018; 124(6):1–7.

14. Al-Ammar K, Hashim A, Husaien M. Synthesis and study of optical properties of (PMMA-CrCl2) composites. cme. 2013;1(3):85–87.

15. Kumar M, Shanmuga Priya N, Kanagaraj S, et al. Melt rheological behavior of PMMA nanocomposites reinforced with modified nanoclay. Nanocomposites. 2016;2(3):109–116.

16. Huang X, Brittain WJ. Synthesis and characterization of PMMA nanocomposites by suspension and emulsion polymerization. Macromolecules. 2001; 34(10):3255–3260.

17. Tan W. K, Yokoi A, Kawamura G, et al. PMMA-ITO composite formation via electrostatic assembly method for infra-red filtering. Nanomaterials (Basel, Switzerland). 2019;9(6):886.

18. Borysiuk VN, Mochalin VN, Gogotsi Y. Molecular dynamic study of the mechanical properties of two-dimensional titanium carbides $Ti_{n+1}C_n$ (MXenes). Nanotechnology. 2015;26(26):265705.

19. Lipatov A, Lu H, Alhabeb M, et al. Elastic properties of 2D Ti3C2Tx MXene monolayers and bilayers. Sci Adv. 2018;4(6):eaat0491.

20. Huang X, Wang R, Jiao T, et al. Facile preparation of hierarchical AgNP-loaded MXene/Fe3O4/polymer nanocomposites by electro-spinning with enhanced catalytic performance for wastewater treatment. ACS Omega. 2019;4(1):1897–1906.

21. Wang Y, Wang J, Han G, et al. Pt decorated Ti_3C_2 MXene for enhanced methanol oxidation reaction. Ceramics Int. 2019;45(2):2411–2417.

22. Lv TY, Min L, Niu F, et al. Wrinkle-structured MXene film assists flexible pressure sensors with superhigh sensitivity and ultrawide detection range. Nanocomposites. 2022;8(1):81–94. Chicago,

23. Sliozberg Y, Andzelm J, Hatter CB, et al. Interface binding and mechanical properties of MXene-epoxy nanocomposites. Compos Sci Technol. 2020;192: 108124.

24. Wan YJ, Li XM, Zhu PL, et al. Lightweight, flexible MXene/polymer film with simultaneously excellent mechanical property and high-performance electromagnetic interference shielding. Composites Part A. 2020;130:105764.

25. Gong K, Zhou K, Qian X, et al. MXene as emerging nanofillers for high performance polymer composites: a review. Composites Part B. 2021;217:108867.

26. Echols IJ, An H, Yun J, et al. Electronic and optical property control of polycation/MXene layer-by-layer assemblies with chemically diverse MXenes. Langmuir. 2021;37(38):11338–11350.

27. Xiantao J, Kuklin AV, Baev A, et al. Two-dimensional MXenes: from morphological to optical, electric, and magnetic properties and applications. Physics Reports. 2020;848:1–58.

28. Enyashin AN, Ivanovskii AL. Two-dimensional titanium carbonitrides and their hydroxylated derivatives: structural, electronic propertis and stability of MXenes Ti3C2 − xNx(OH)2 from DFTB calculations. J Solid State Chem. 2013;207:42–48.

29. Sang X, Xie Y, Lin MW, et al. Atomic defects in monolayer titanium carbide (Ti3C2T x) MXene. ACS Nano. 2016;10(10):9193–9200.

30. Lei L, Xiaoya L, Jianfeng W, et al. Corrigendum to new application of MXene in polymer composites toward remarkable antidripping performance for flame retardancy. Composites Part A. 2022; 157: 106932.

31. Zhao J, Yang Y, Yang C, et al. A hydrophobic surface enabled salt-blocking 2D Ti3C2 MXene membrane for efficient and stable solar desalination. J Mater Chem A. 2018;6(33):16196–16204.

32. Xinxin S, Yanfeng Z, Li Z, et al. Properties of two-dimensional Ti_3C_2 MXene/thermoplastic polyurethane nanocomposites with effective reinforcement via melt blending. Compos Sci Technol. 2019;181: 107710.

33. Tao L, Bing D, Jie W, et al. Sandwich-structured ordered mesoporous polydopamine/MXene hybrids as high-performance anodes for lithium-ion batteries. ACS Appl Mater Interfaces. 2020;12(13): 14993–15001.

34. Zhang Y, Wang L, Zhang J, et al. Fabrication and investigation on the ultra-thin and flexible $Ti_3C_2T_x$/co-doped polyaniline electromagnetic interference shielding composite films. Compos Sci Technol. 2019;183:107833.

35. Haq YU, Murtaza I, Mazhar S, et al. Investigation of improved dielectric and thermal properties of ternary nanocomposite PMMA/MXene/ZnO fabricated by in-situ bulk polymerization. J Appl Polym Sci. 2020;137(40):e49197.

36. Stojanovic D, Orlovic A, Glisic SB, et al. Preparation of MEMO silane-coated SiO2 nanoparticles under high pressure of carbon dioxide and ethanol. J Supercrit Fluids. 2010;52(3):276–284.

37. Biswas S, Alegaonkar PS. MXene: evolutions in chemical synthesis and recent advances in applications. Surfaces. 2021;5(1):1–36.

38. Pešić J, Šolajić A, Mitrić J, et al. Structural and optical characterization of titanium–carbide and polymethyl methacrylate based nanocomposite. Opt Quantum Electron. 2022;54(6):1–13.

39. Riazi H, Anayee M, Hantanasirisakul K, et al. Surface modification of a MXene by an aminosilane coupling agent. Adv Mater Interfaces. 2020;7(6): 1902008.

40. Ahmad S, Ahmad S, Agnihotry SA. Synthesis and characterization of in situ prepared poly (methyl methacrylate) nanocomposites. Bull Mater Sci. 2007; 30(1):31–35.

41. Doğan S, Özcan T, Doğan M, et al. The effects on antioxidant enzymes of PMMA/hydroxyapatite nanocomposites/composites. Enzyme Microb Technol. 2020;142:109676. 109676,

42. Dong Y, Sang D, He C, et al. Mxene/alginate composites for lead and copper ion removal from aqueous solutions. RSC Adv. 2019;9(50):29015–29022.

43. Djire A, Zhang H, Liu J, et al. Electrocatalytic and optoelectronic characteristics of the two dimensional titanium nitride $Ti_4N_3T_x$ MXene. ACS Appl Mater Interfaces. 2019;11(12):11812–11823.

44. Natu V, Clites M, Pomerantseva E, et al. Mesoporous MXene powders synthesized by acid induced crumpling and their use as na-ion battery anodes. Mater Res Lett. 2018;6(4):230–235.

45. Zhao MQ, Xie X, Ren CE, et al. Hollow MXene spheres and 3D macroporous MXene frameworks for Na-ion storage. Adv Mater. 2017;29(37): 1702410.

46. Woo JH, Kim NH, Kim SI, et al. Effects of the addition of boric acid on the physical properties of MXene/polyvinyl alcohol (PVA) nanocomposite. Composites Part B. 2020;199:108205.

47. Ali Sabri B, Satgunam M, Abreeza N, et al. A review on enhancements of PMMA denture base material with different nano-fillers. Cogent Eng. 2021;8(1):1875968.

48. Jimmy J, Kandasubramanian B. Mxene functionalized polymer composites: synthesis and applications. Eur Polym J. 2020;122:109367.

49. Sellam C, Zhai Z, Zahabi H, et al. High mechanical reinforcing efficiency of layered poly(vinyl alcohol) – graphene oxide nanocomposites. Nanocomposites. 2015;1(2):89–95.

50. Kłysz S, Lisiecki J. Selected problems of measurement uncertainty – part I. Tech Sci. 2008;11(1): 253–264.

51. Kłysz S, Lisiecki J. Selected problems of measurement uncertainty – part II. Tech Sci. 2008;11(1): 265–276.

52. Podgornik B, Žužek B, Sedlaček M, et al. Analysis of factors influencing measurement accuracy of al alloy tensile test results. Meas Sci Rev. 2016;16(1):1–7.

53.　Maleski K, Mochalin VN, Gogotsi Y. Dispersions of two-dimensional titanium carbide MXene in organic solvents. Chem Mater. 2017;29, 4:1632–1640.

54.　Desai ML, Basu H, Singhal RK, et al. Ultrasmall two dimensional MXene nanosheets for selective and sensitive fluorescence detection of ag + and Mn2+ ions. Colloids Surf A. 2019;565: 70–77.

55.　Zhang Q, Wang F, Zhang H, et al. Universal Ti3C2 MXenes based Self-Standard ratiometric fluorescence resonance energy transfer platform for highly sensitive detection of exosomes. Anal Chem. 2018;90(21):12737–12744.

56.　Abozaid RM, Lazarević ZŽ, Radović I, et al. Vesna Radojević, optical properties and fluorescence of quantum dots CdSe/ZnS-PMMA composite films with interface modifications. Opt Mater. 2019;92:405–410.